CERN-ATS-Note-2012-017 MD

April 2012
massimo.giovannozzi@cern.ch

IR2 aperture measurements at 3.5 TeV

C. Alabau Pons, G. Arduini, R.W. Assmann, R. Bruce, M. Giovannozzi, J.M. Jowett, E. MacLean, G. Müller, S. Redaelli, R. Tomás, G. Valentino, J. Wenninger

Keywords: triplet aperture, IR2, local bump, tune and coupling

Summary

Aperture measurements in the ALICE interaction region were carried out to determine a safe configuration of β^* and crossing angle for the 2011 heavy ion run. Proton beams were used at the end of the proton run, after the commissioning of the squeeze to $\beta^* = 1$ m in IR2. In this paper, the results of aperture measurements are summarised and the final collision configuration is presented. Results of parasitic measurements of the effect of non-linear triplet fields with large orbit bumps in the IRs are also summarised.

Contents

1 Introduction **2**

2 Strategy and beam conditions **3**
2.1 Beam conditions and measurements 3
2.2 Measurement technique 4
2.3 IR bumps and collimator alignment 4

3 Measurement results **7**

4 Tune and Coupling Measurements with large bumps in the triplets **9**

5 Conclusions **11**

1 Introduction

The 2011 LHC proton run was followed by 4 weeks of lead ion operation at an energy of $3.5\,Z$ TeV/beam. In keeping with the the low proton luminosity requirements of ALICE, the interaction point (IP) 2 had been kept at the injection optics ($\beta^* = 10\,\mathrm{m}$) during proton physics. To maximise Pb-Pb luminosity in ALICE, β^* had to be reduced for the Pb-Pb operation. In addition ALICE preferred to have a small, ideally zero, net crossing angle, $p_{yc} = 0$, [1] in order to avoid shadowing of portions of the spectator neutron flux at the Zero-Degree Calorimeters (ZDCs). Since high luminosity was the first priority, crossing angles satisfying $|p_{yc}| < 60\,\mu\mathrm{rad}$ were acceptable provided $\beta^* = 1\,\mathrm{m}$ could be achieved [2].

Since the ALICE spectrometer magnet and its compensating correctors are always operated at the same value of the magnetic field (except that its polarity may be reversed), the crossing angle at IP2 is given by

$$p_{yc}(\mathrm{IP2}) = \pm\frac{490\,\mu\mathrm{rad}}{E/[Z\ \mathrm{TeV}]} + p_{y\mathrm{ext}}(\mathrm{IP2}) \tag{1}$$

where$p_{y\mathrm{ext}}$ is the "external" crossing angle and the first term is the "internal" angle from the spectrometer. At 3.5 TeV the latter is $\pm 140\,\mu\mathrm{rad}$ and can be cancelled with $p_{y\mathrm{ext}} = \mp 140\,\mu\mathrm{rad}$. Precise measurements of the aperture in the interaction region (IR) are essential to determine the acceptable range of $p_{y\mathrm{ext}}$ for a given β^*. Since small β^* implies larger beams in the triplet quadrupoles and tighter bounds on $p_{y\mathrm{ext}}$.

Note that the proton run was carried out with $p_{y\mathrm{ext}} = 80\,\mu\mathrm{rad} \Rightarrow p_{yc} = 60\,\mu\mathrm{rad}$ (for the positive spectrometer polarity).

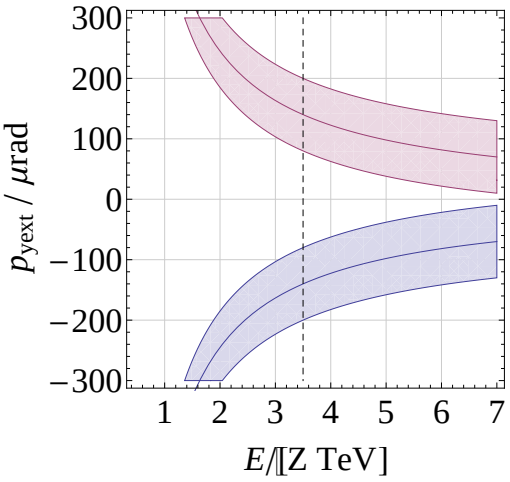

Figure 1: Allowed range of the vertical external crossing angle at IP2 as a function of beam energy. The lower/upper branch of the region corresponds to positive/negative spectrometer polarity (positive spectrometer polarity contributes a positive angle for Beam 1 at IP2). The solid lines correspond to zero vertical crossing angle at IP2.

Earlier, during the proton run, aperture measurements in IP1 and IP5 [3] had shown that these IPs could be set to $\beta^* = 1\,\mathrm{m}$ with a crossing angle of $120\,\mu\mathrm{rad}$. Following these encouraging results, it was decided to commission the squeeze down to $\beta^* = 1\,\mathrm{m}$ in IP2 also. The commissioning of this new optics was followed by measurements of the IR2 aperture at $\beta^* = 1\,\mathrm{m}$, for various values of of the crossing angles. To leave time to deal with any aperture problems and prepare new settings before the ion run, these measurements were started before the end of the proton run, ie, before the last MD block and the final Technical Stop of 2011. This note presents the results.

Table 1: Beam parameters and machine configuration for the measurements.

Beams required	Both beams
Beam energy [GeV]	3500
β^* in IP2 [m]	1.0
β^* in IP1/IP5 [m]	1.0
β^* in IP8 [m]	3.0
External crossing IP2 [μrad]	-80 and $+120$ (two separated measurements)
External crossing IP1/IP5 [μrad]	± 120
External crossing IP8 [μrad]	-250
Parallel separation [mm]	0.7 in all IPs
Particle species	protons
Bunch intensity [10^9 p]	< 10
Number of bunches	1 per beam
Transv. emittance [μm]	3-5
Orbit change	Various types of bump added to the nominal orbit
Collimator configuration	Tertiary collimators in IR2 moved, no change in any other IR
Feedback configuration	OFB and QFB off at the end of the squeeze
Special conditions	Alignment of TCTs in IP2 required in absences of a well established orbit reference

It includes a short description of the beam conditions and procedure to measure the aperture safely The results determine the final crossing angle configuration for the ion physics run. The overall commissioning of the squeeze in IP2 is presented in detail in a companion note [4]. The large local bumps used to measure aperture in the triplet region are also well suited to probe the effects of non-linear field components of the triplet magnets and these results are also presented.

2 Strategy and beam conditions

2.1 Beam conditions and measurements

The main beam and machine parameters for the aperture measurements are listed in Tab. 1. For safety, single bunches with intensities below 10^{10} p and blown-up transverse emittances were used. The IR2 measurements were done with IP1, IP5 and IP8 squeezed to the operational values of β^* for proton physics. For operational reasons, the squeeze in IP2 is executed after those of the other IPs, adding a total of 775 s to the overall squeeze duration. Measurements were performed with beams separated horizontally by $\pm 0.7\,\mathrm{mm}$ because this is the condition of tightest aperture in the separation plane.

Aperture measurements were carried out with proton beams on 29 October and again during the MD4 block on 2 November 2011 (see Table 2):

1. About 4 h at the end of a fill for squeeze commissioning and optics measurements. The initial bunch intensities were higher than 10^{10} p and the normalised emittances below $2\,\mu\mathrm{m}$. The beams were therefore blown up with the AC dipole to achieve safer beam conditions. This first measurement was carried out with the nominal external crossing angle for proton physics of $-80\,\mu\mathrm{rad}$. Note that the final optics corrections were put in place before the aperture measurements.

Table 2: Information about the two IR2 aperture measurement campaigns.

Date	Fill	Planes	Initial Crossing	Time	Remarks
29/10/2011	2263	H + V	$-80\,\mu$rad	4 h	Measurements performed after squeeze commissioning, AC dipole blowup
02/11/2011	2272	V	$+120\,\mu$rad	3 h	Dedicated fill with probe beams

2. A further 3 h during a dedicated fill, with $p_{y\text{ext}} = +120\,\mu$rad to probe the aperture on the opposite side. Initial beam parameters for this fill were optimum for the measurements and no beam manipulation was needed at top energy.

The measured beam currents for the two fills are shown in Fig.2. The times quoted do not include set-up and tertiary collimator alignment.

Contrary to previous measurements in IP1 and IP5 [3], the aperture was measured separately for the two beams. This approach followed initial scans done with both beams together, which indicated aperture restrictions on the left side of IP2.

2.2 Measurement technique

The details of the operational procedure for aperture measurements are given in [3, 5]. Further crossing orbit bumps are superposed on the initial crossing and separation schemes (see Fig. 3). The bump amplitude is increased until the beam touches the tertiary collimators (TCTs) that protect the triplet magnets. These collimators are initially set to 11.8σ. Then, (1) the TCTs are opened symmetrically around the closed orbit in steps of 0.5σ and (2) the bump is increased in steps equivalent to a 0.25σ offset at the TCTs, so that the beam once again touches the collimators after 2 orbit steps. The actions (1) and (2) are repeated iteratively until the beam touches a loss location different from the TCTs, eg, the triplet magnets. In these conditions, it is possible to determine the collimator aperture above which local bottlenecks are not protected by the collimators (a). The absolute orbit measurements with this maximum orbit excursion, ie, with the beam touching the aperture bottleneck, provide quantitative measurements of the mechanical aperture (b), provided that the loss location is identified precisely.

The exact shape of the bump used to steer the beams into the aperture can bias the results and this effect must be taken into account in off-line analysis. On the other hand, previous measurements in other IPs indicated that the errors induced by taking into account the approach (a) only are small [3]. The full analysis taking into account the orbit excursion in millimetres will also be carried out.

2.3 IR bumps and collimator alignment

The bumps used for probing the IR2 aperture are shown in Figure 4. These bumps further increase the crossing angle in the interaction point. The sign of the bump is chosen to probe the most critical locations for the configuration of the nominal schemes, see Figure 3. Initially, measurements were done with the standard knobs used in operation to optimise the IP beam angle in physics ("luminosity" crossing angle, see left graphs of Fig. 4). However, the strength of the orbit correctors was insufficient to reach the aperture with these bumps alone. To increase the orbit excursion, additional crossing bumps were built with correctors of cells further from the IP (right graphs of Fig. 4). An example of the absolute orbit simulated for the case with an additional crossing angle added to the unperturbed orbit is given in Fig. 5. In this example, both beams are trimmed to the same value, whereas in the measurements they were trimmed separately.

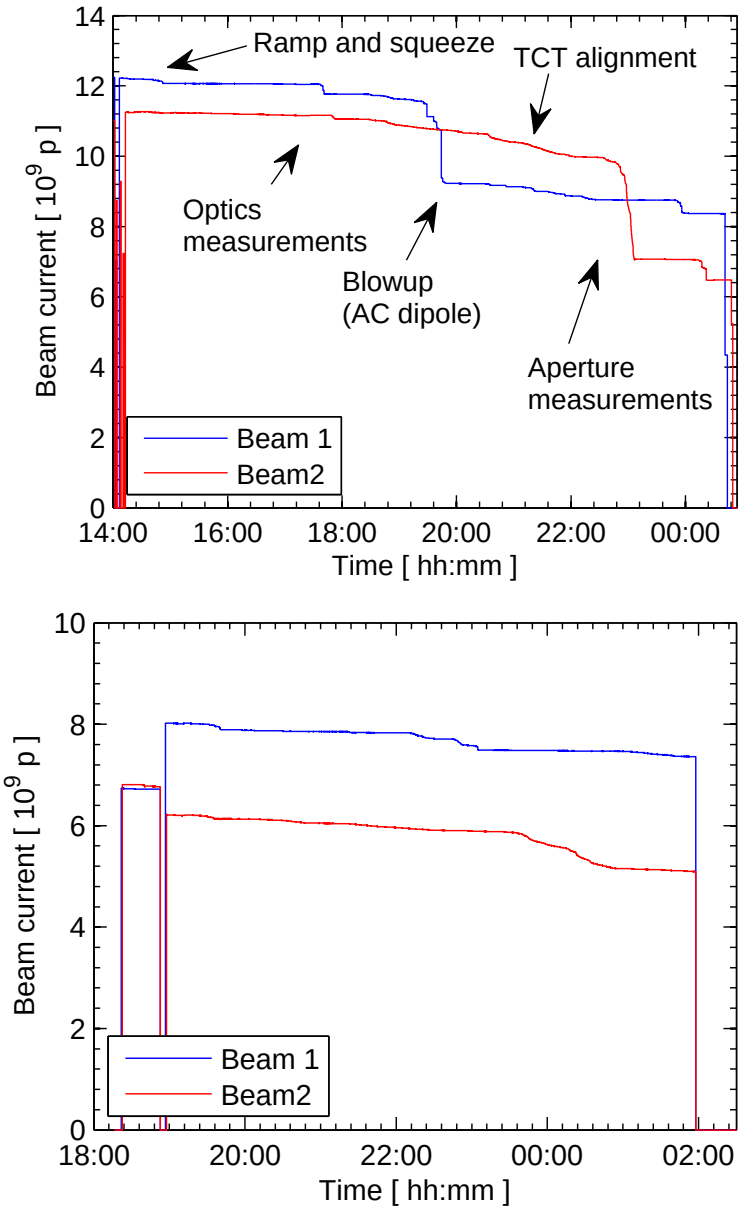

Figure 2: Beam current as a function of time measured during the two aperture measurements: 29 October (top) and 2 November 2011 (bottom).

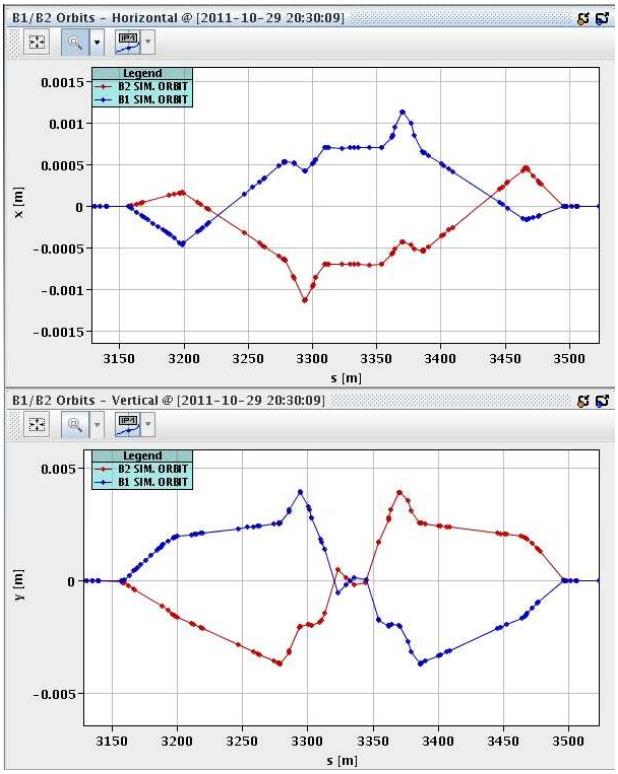

Figure 3: Nominal separation (top) and crossing (bottom) bumps in IP2. The horizontal and vertical closed orbit is given as a function of the longitudinal coordinate.

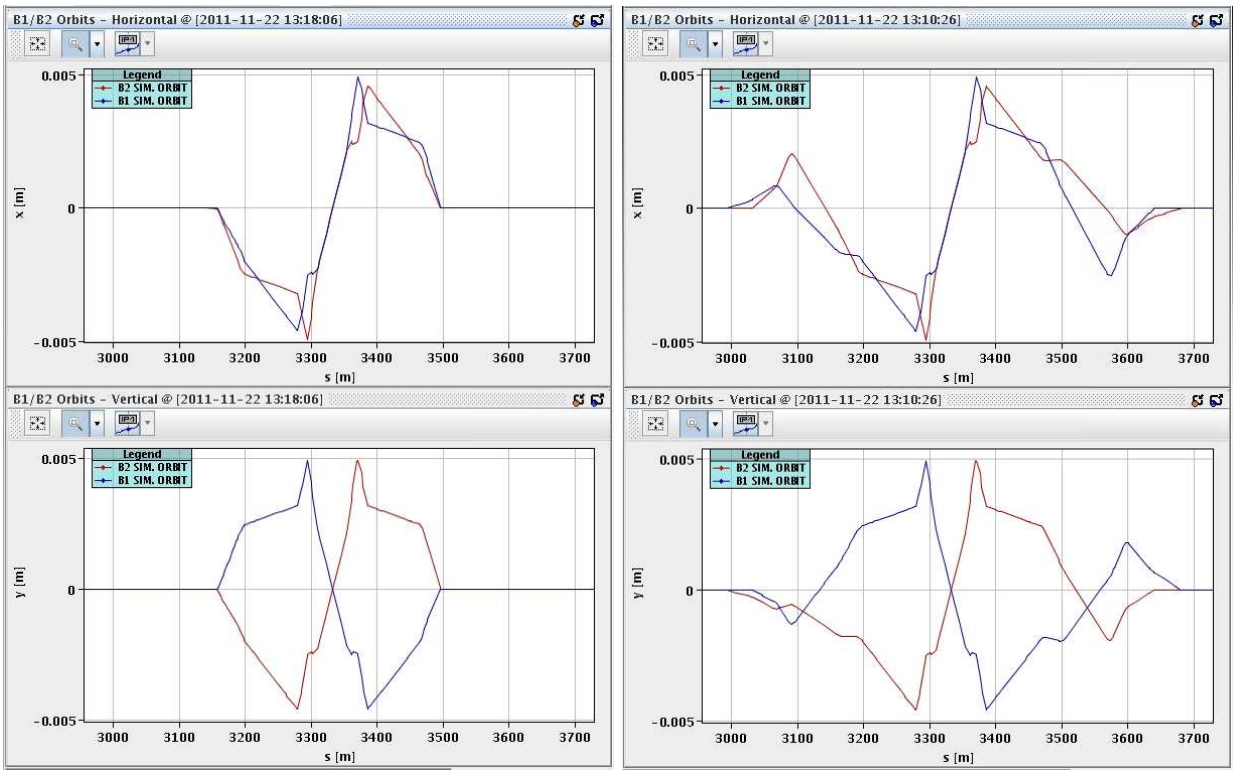

Figure 4: Additional crossing angle bumps used to probe the IR2 aperture: crossing knobs for luminosity optimisation (left) and additional external crossing angle (right). The horizontal (top) and vertical (bottom) closed orbit is given as a function of the longitudinal coordinate. In this example both knobs are matched to provide an additional angle of $100\,\mu\mathrm{rad}$ at IP2.

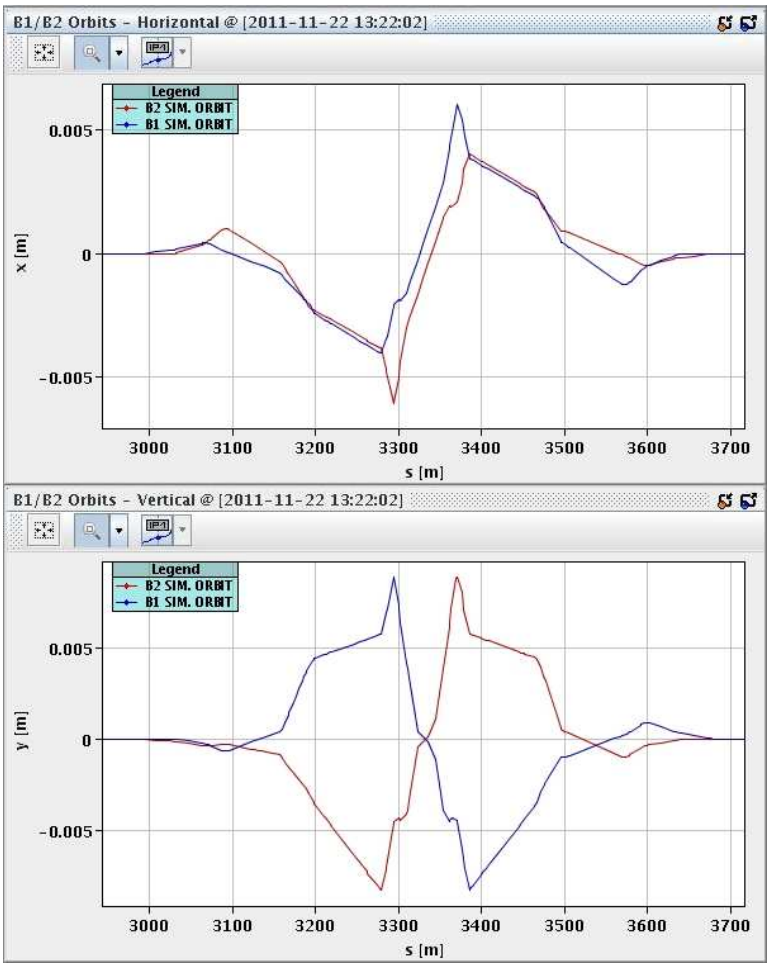

Figure 5: Example of total aperture bump in IP2 when the additional crossing bumps of Fig. 4 are added to the nominal bumps of Fig. 3. The horizontal (top) and vertical (bottom) closed orbit is given as a function of the longitudinal coordinate. Each aperture knob is matched to a 50 μrad change at the IP.

This measurement technique relies on a good initial alignment of the tertiary collimators around the beam orbit ("beam-based alignment"). This had not yet been set up for the new optics at the time of the measurements. Therefore, the TCTs were aligned as a part of each aperture measurement, for each considered value of separation and external crossing angles (see Tab. 2). The beam-based centres of the tertiary collimators in the various configurations are summarised in Table 3. For each measurement, the TCT collimators were then set to 12σ around the these centres, corresponding to half gaps of 9.12 mm (H) and 11.1 mm (V).

For reference, in Table 4 the shift of the collimator's centre between the configuration corresponding to $+120$ μrad and -120 μrad is reported as computed from beam-based data, the theoretical model, or the YASP interpolated orbit. The agreement is clearly remarkable.

3 Measurement results

The results of aperture measurements for both beams in terms of TCT half-gaps in units of nominal beam σ are summarised in Tab. 5. The quoted numbers indicate the TCT gap above which IR aperture bottlenecks were exposed. The results are given both for the separation and the crossing planes.

Table 3: Summary of beam-based collimator centres measured in the various machine conditions. The configuration for $120\,\mu\mathrm{rad}$ was prepared but the beams were dumped before the aperture measurements.

Crossing angle [μrad]	Beam	Collimator name	Beam-based centre [mm]
-80	B1	TCTH.4L2.B1	-0.59
-80	B2	TCTH.4R2.B2	-0.73
-80	B1	TCTVB.4L2	3.50
-80	B2	TCTVB.4R2	2.73
$+120$	B1	TCTVB.4L2	-2.56
$+120$	B2	TCTVB.4R2	-3.58
-120	B1	TCTVB.4L2	4.73
-120	B2	TCTVB.4R2	3.65

Table 4: Comparison of the shift of the collimator's centre for configurations corresponding to ± 120 μrad as derived from the beam-based alignment, the theoretical model, and the interpolation of the YASP data. The agreement is remarkable.

Beam	Collimator name	Beam-based centre [mm]	Model centre [mm]	YASP centre [mm]
B1	TCTVB.4L2	7.29	7.20	7.20
B2	TCTVB.4R2	7.23	7.20	7.04

In general, the aperture is larger than $15\,\sigma$, except for the Beam 1 case with $+120$ μrad of external crossing angle. This configuration features an abnormally low aperture of only $12.5\,\sigma$ for the injected beam, i.e., Beam 1.

Table 5: IR2 aperture in sigma units derived from the opening of tertiary collimators.

Crossing angle [μrad]	Beam	Plane	Type of bump in standard optics	Aperture [σ]
-80	B1	H	Separation	16.0-16.5
-80	B2	H	Separation	15.5-16.0
-80	B1	V	Crossing	15.5-16.0
-80	B2	V	Crossing	16.0-16.5
$+120$	B1	V	Crossing	12.5-13.0
$+120$	B2	V	Crossing	15.0-15.5

The expected scaling of the available aperture, generated by the unexpected bottleneck, as a function of the crossing angle is given in Fig. 6 for various values of β^*. These calculations assume a $12.5\,\sigma$ aperture at the TCTVB, as found in the measurements.

The scaled aperture accounts for the change in beam size with $\beta^*$and the change in orbit from the crossing angle, where it is assumed that the crossing bump shape remains constant during the squeeze, which is correct in this context.

A different analysis can be performed and is presented in Table 6. From the knowledge of the extreme orbit and that of the corresponding TCT opening the actual size of the beam envelope can be derived such that the measured aperture in millimetres can be obtained.

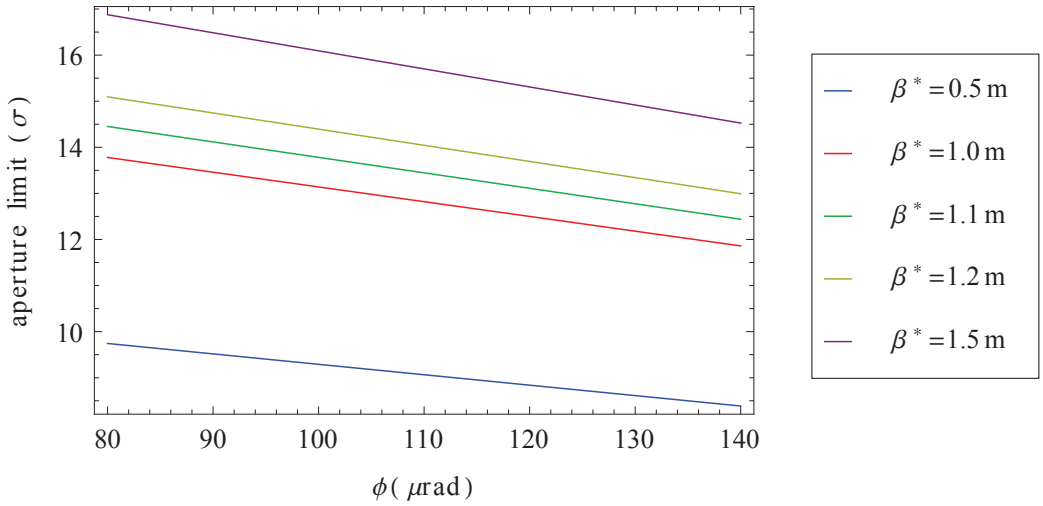

Figure 6: Simulated scaling of available aperture as a function of the IR2 crossing angle for different β^* values. The starting point is the value of the observed aperture bottleneck corresponding to $12.5\ \sigma$ for β^*1 m and a crossing angle of $+120\ \mu$rad.

In Table 6 the extreme orbit amplitude is quoted as well as the derived beam envelope, which are then used to derived the measured aperture. The design aperture is also quoted. There are cases for which the dominant beam losses appear upstream of the TCTVB and for these specific cases the last column of Table 6 provides the element name where the beam edge is nearest to the mechanical aperture.

In Fig. 7 the extreme trajectories in the crossing plane for $-80\ \mu$rad and $+120\ \mu$rad, respectively are shown. The left graphs represent Beam 1, while those on the right the situation of Beam 2. The orbits are obtained by interpolation of the measured ones and the reported beam envelope is computed at $4\ \sigma$ only for the sake of comparison.

It is worthwhile reporting the observed impact of the TCDD.4L2 opening on the losses measured by the BLMs in IR2 (see Fig. 8). Indeed, whenever the TCDD.4L2 is in its nominal configuration non-negligible losses are observed on the D2.L2, thus requiring to open up the jaws for avoid any perturbation of the aperture measurements.

The situation concerning the aperture scans in the vertical plane for Beam 1 can be found in Fig. 9. two groups of three pictures are shown and each group reports the evolution of the beam losses (upper graph), the orbit change at Q3.R2 (centre graph), and jaw position of the TCTVB.4R2 (lower graph). The first group refers to the first initial aperture scan, with the TCDD.4L2 still in the nominal position, while the second block reports the situation after opening the TCDD.4L2. It is clearly seen that, in spite of the rather large range of values for the orbit and jaw's position, no losses other than at the location of the TCTVB.4R2 have been observed, thus indicating the presence of an aperture restriction in the region upstream of the tertiary collimator.

4 Tune and Coupling Measurements with large bumps in the triplets

An off-axis beam travelling through the IR will undergo a tune shift on encountering non-linear fields, due to feed down to either normal gradient or linear coupling. In principle therefore, by observing tune and coupling under the influence of an orbit bump it is possible to identify non-linear errors in the IR magnets: Table 7 displays the principal measurable feed down for specific multipoles

Table 6: Maximum orbit excursion and envelope width achieved during aperture measurements corresponding to losses occurring at locations other than the TCTs. The design aperture is also given. For the cases marked with †, unexpected bottlenecks upstream of the TCTVB are limiting the aperture. These unexpected loss locations are therefore not located at the indicated elements with largest orbit excursion. For the case ††, the envelope was re-computed from the TCT collimator gaps during the alignment.

Crossing angle [μrad]	Beam/ Plane	Total Orbit [mm]	Envelope width [mm]	Total aperture [mm]	Design aperture [mm]	Element name
-80	B1/H	$+22.8$	7.4	$+23.8$	25	MCBXH.2R2†
-80	B2/H	-17.3	5.8	-23.1	25	MQXB.B2L2
-80	B1/V	$+18.6$	6.0	$+24.6$	30	MQXB.B2L2†
-80	B2/V	$+18.5$	7.3	$+25.8$	30	MCBXV.2R2†
$+120$	B1/V	$+15.7$	7.4	$+23.1$	30	MQXA.3R2†
$+120$	B2/V	-17.5	6.9††	-24.4	30	MCBXV.2R2††

and bumps. As described in [12] observations of the tune (with controlled coupling) under the influence of selected IR bumps have formed a successful basis for non-linear optics corrections at RHIC.

Table 7: Normal gradient (ΔQ) / Coupling (ΔC) feed down from non-linear Multipoles

	$\mathbf{b}_3$	$\mathbf{a}_3$	$\mathbf{b}_4$	$\mathbf{a}_4$	$\mathbf{b}_5$	$\mathbf{a}_5$	$\mathbf{b}_6$
H bump	ΔQ	ΔC	ΔQ	ΔC	ΔQ	ΔC	ΔQ
V bump	ΔC	ΔQ	ΔQ	ΔC	ΔC	ΔQ	ΔQ

Throughout the IR2 aperture scans parasitic measurements of both tune and coupling as a function of the applied orbit bump were performed. Similar studies have been conducted for IR1 and IR5 [3].

Measurements were performed using the continuous FFT BBQ system.

Figure 10 (upper graphs) shows the raw tune and coupling measurements taken during the aperture MD of 29th of October. At ∼21:45 it was necessary for the chirp to be turned off to facilitate the aperture measurements, and a corresponding decrease in the data quality is apparent, however there is still clear evidence of the existence of higher order multipoles in the IR. Most notable is the significant increase in the coupling during the Horizontal angle scans of Beam 1 (∼23:32 - ∼00:04) and Beam 2 (∼00:10 - ∼00:30). Prior to the chirp being turned off, there is some clear data for both beams during the vertical scan, several jumps in the Beam 1 coupling after the chirp was deactivated are also visible at around 22:00 and 22:30 however the Beam 2 data is more obscure.

During the aperture measurement on the 2nd of November the tunes and coupling were again measured; the data however, as shown in figure 10 (lower graphs), is low quality. During some moments when the chirp was active it is possible to see the effect of the trims on the coupling and tunes, however for the most part any trends are obscured. It may be possible to improve upon this situation by cleaning and averaging the data within the trim plateaus.

In addition to the IR2 aperture measurements, it was also possible to repeat this procedure during an end-of-fill test of the setup following the ALICE spectrometer polarity reversal on 24 November. Contrary to the measurements performed on the 29th of October and the 2nd of November, during

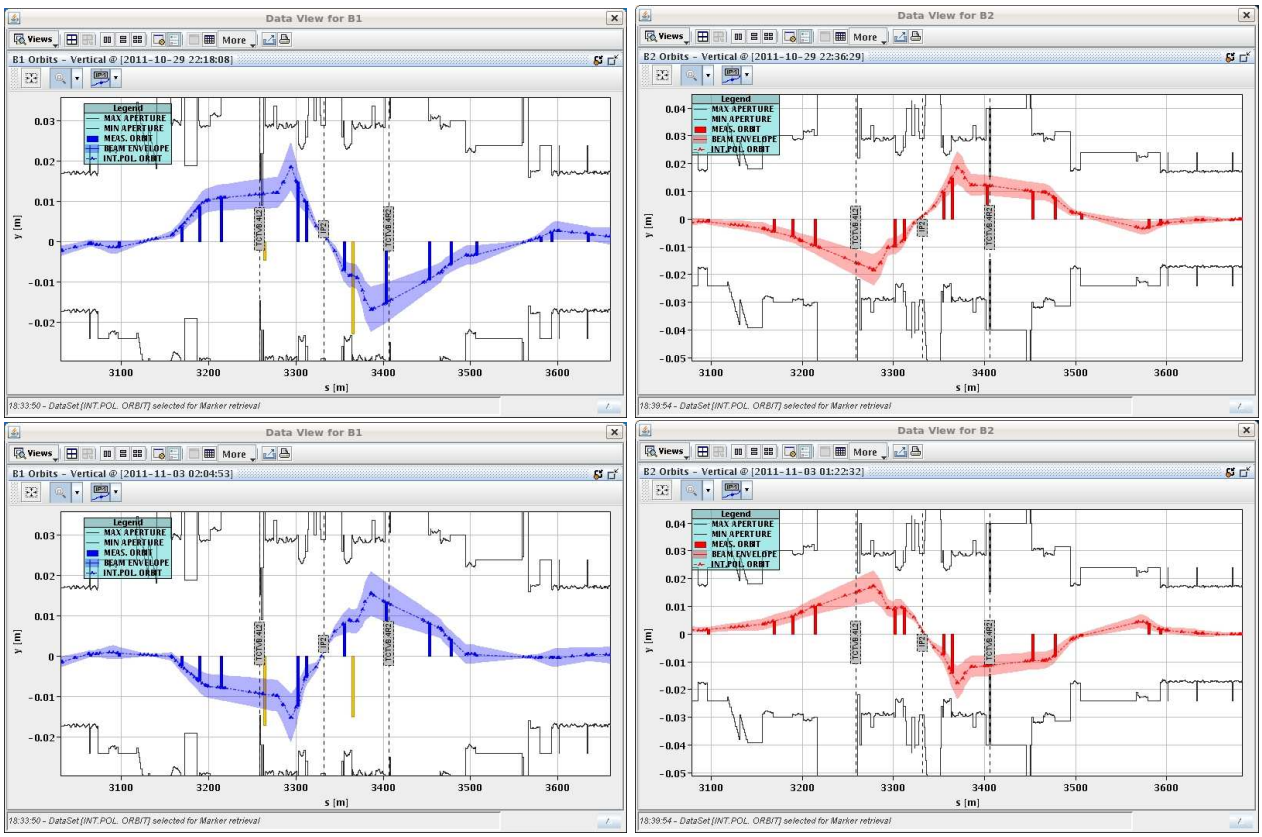

Figure 7: Interpolated vertical orbit as a function of the longitudinal coordinate in IP2 for the extreme cases when the beam touched the aperture. The initial external crossing angle was $-80\,\mu\mathrm{rad}$ (upper row) and $120\,\mu\mathrm{rad}$ (lower row), respectively. The Beam 1 (left column) and Beam 2 (right column) cases are given. A $4\,\sigma$ beam envelope is added to the orbit for reference.

the ALICE spectrometer polarity reversal beams consisted of many high intensity ion bunches ($\sim 6.2 \times 10^9$ charges/bunch) and were in collision in IRs 1 and 5.

On this occasion the vertical crossing angle was taken from $-80°$ to $+80°$ in $10°$ steps. It was also possible to have the chirp active throughout the operation. The data, as seen in figure 11, is of a very high quality.

A bump in the Beam 2 coupling data is observed at ∼15:20-15:25, which coincides approximately with the chirp being turned briefly off and then on. However as the measurement performed is the absolute coupling the observed bump could also be the result of the coupling becoming negative between 15:20 and 15:25. A similar jump was observed at 15:20 for Beam 1, however no shift was seen around 15:25 when the chirp was turned back on.

These three sets of beam based measurements should now be analysed as a function of the applied crossing angle trims and compared to simulation in order to attempt to identify higher order multipoles present in IR2, and check the consistency with magnetic error measurements performed on the IR magnets.

5 Conclusions

The aperture in IR2 was measured at 3.5 TeV with the $\beta^* = 1\,\mathrm{m}$ optics, in the crossing and separation planes. The measurements were performed with proton beams with both signs of the external crossing angle, specifically at $p_{y\mathrm{ext}} = -80\,\mu\mathrm{rad}$ and $+120\,\mu\mathrm{rad}$. The measurement results indicate

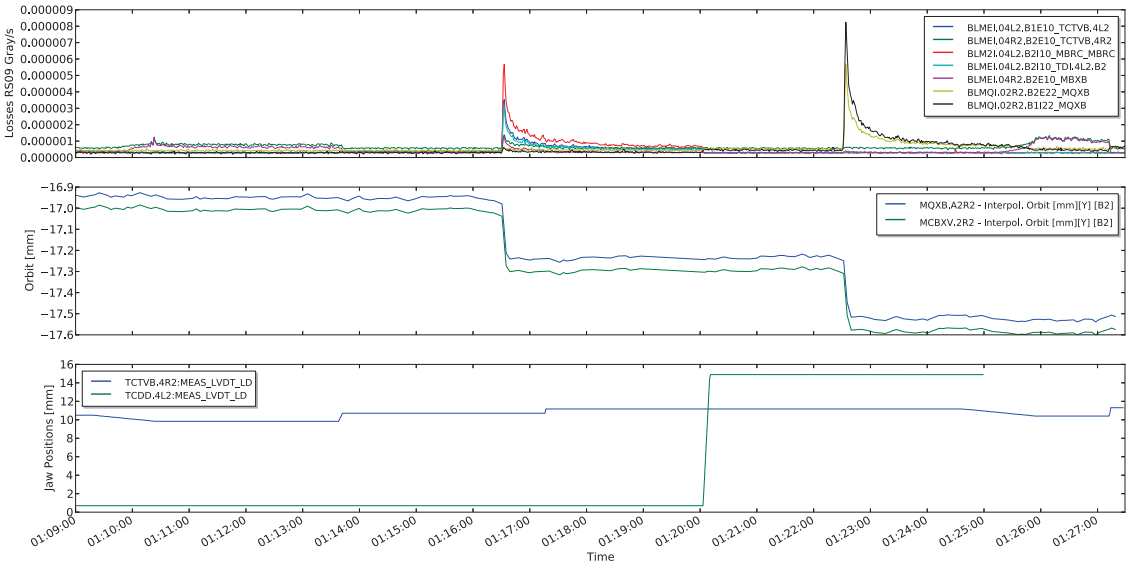

Figure 8: Evolution of beam losses (upper), orbit change at Q2.R2 (centre), and jaw position of the TCTVB.4R2 and TCDD.4L2 (lower). The impact of the TCDD opening on the losses as measured by the BLMs in the region of the D2.R2 is clearly visible.

an unexpected bottleneck in the region between the TDI.4L2 and the TCTVB.4L2, on the left of IR2. For $p_{y\text{ext}} = 120\,\mu\text{rad}$—corresponding to a crossing angle $p_{yc} = 20\,\mu\text{rad}$ at IP2—the measured aperture of 12.5σ does not leave enough margin between the TCT and the triplet aperture with the present relaxed collimator settings. The cases with $p_{y\text{ext}} = \pm 80\,\mu\text{rad}$—corresponding to a crossing angle $p_{yc} = \mp 60\,\mu\text{rad}$ at IP2—do provide acceptable aperture and just satisfy the requirements related to ZDC shadowing. On the basis of these results these last values were chosen as the physics configuration for the 2011 Pb-Pb run.

It is worth mentioning that as a consequence of the results obtained during the second aperture measurement session, it was decided to install additional BLMs in the left side of IP2 in the region between the TCTV and the TDI. However, no beam time was allocated for additional aperture measurements, as visual inspection could be carried out during the winter technical stop and the layout of IR2 was going to be changed in order to alleviate the spectator neutron shadowing at the ZDCs by the TCTs [13].

Acknowledgements

We thank the LHC operations crews for support during the measurements and D. Wollmann for the collimator alignment.

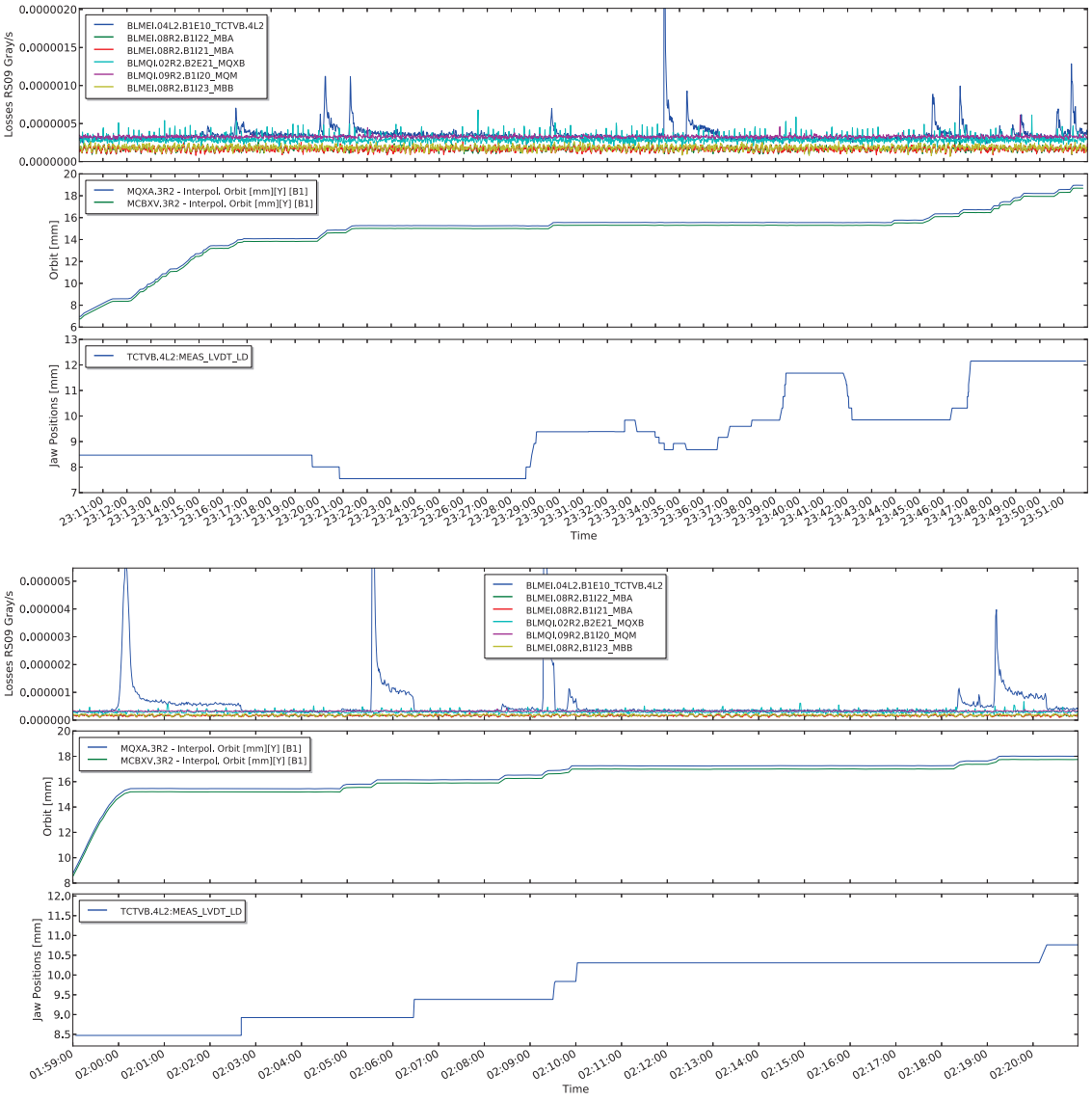

Figure 9: Evolution of beam losses (upper), orbit change at Q3.R2 (centre), and jaw position of the TCTVB.4R2 (lower) for the first vertical aperture scan (first block of three plots) and the second block of aperture scan (second block of three plots) when the TCDD.4L2 was opened. Only losses at the TCTVB.4L2 can be observed in spite of the rather large scan over collimator aperture and orbit value.

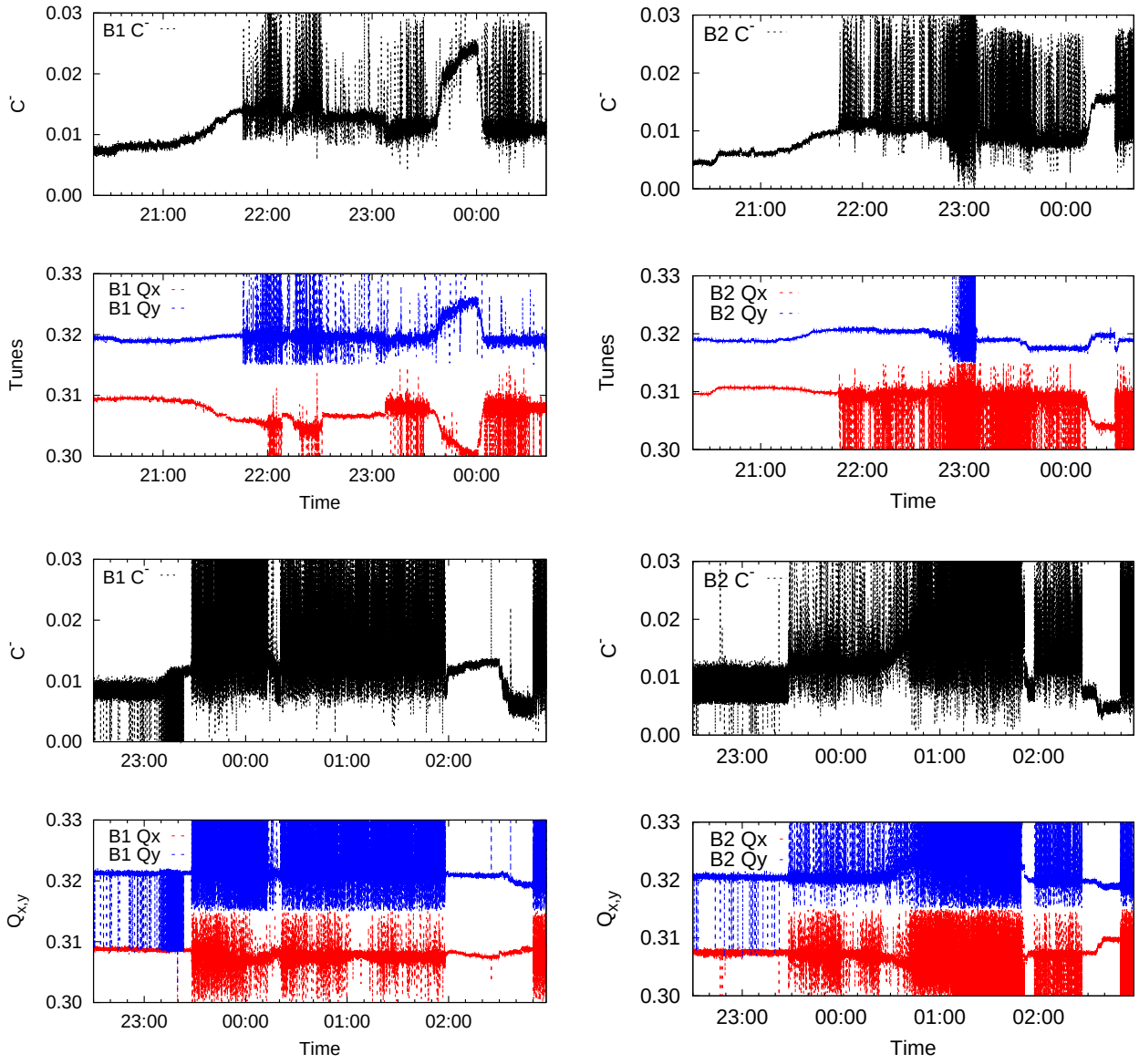

Figure 10: Variation in tune and coupling of Beam 1 (left) and Beam 2 (right) throughout the IR2 aperture scan of the 28th and 29th of October (upper graphs). Variation in tune and coupling of Beam 1 (left) and Beam 2 (right) throughout the IR2 aperture scan of the 2nd and 3rd of November (lower graphs).

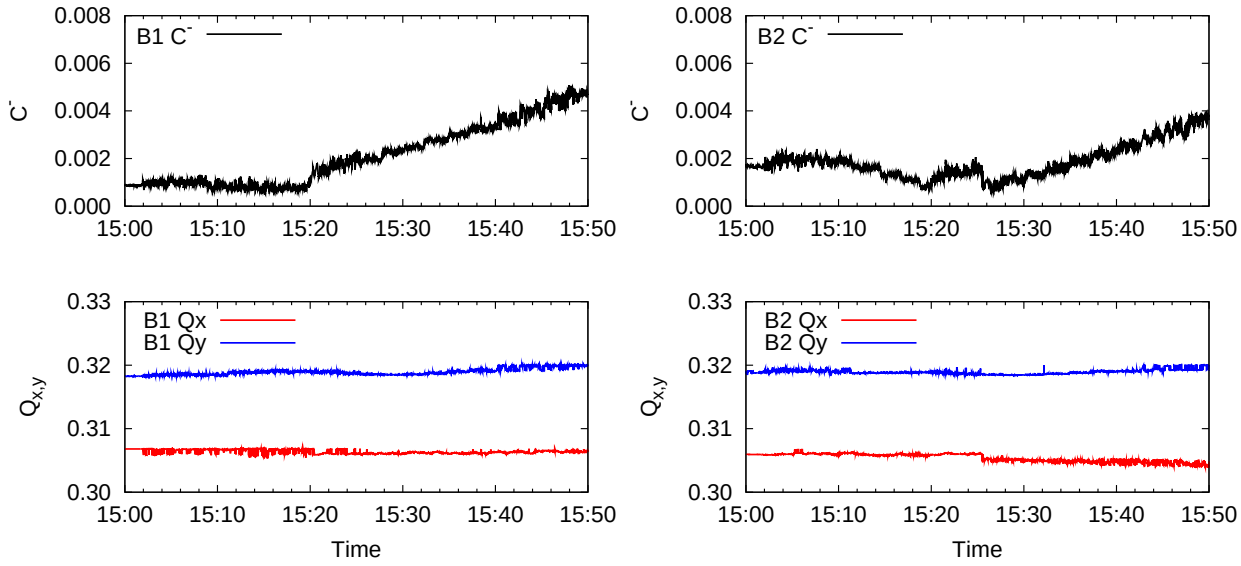

Figure 11: Variation in tune and coupling of Beam 1 (left) and Beam 2 (right) throughout the crossing angle reversal following Alice spectrometer polarity reversal on 24th of November.

References

[1] Minutes of the 113th meeting of the LHC Machine Committee, held on 2 November 2011, https://espace.cern.ch/lhc-machine-committee/Minutes/1/lmc_113.pdf, slides by J. Wenninger, J.M. Jowett and several earlier discussions.

[2] M. Ferro-Luzzi, private communication.

[3] C. Alabau Pons, R. Assmann, R. Bruce, M. Giovannozzi, E. MacLean, G. Müller, S. Redaelli, F. Schmidt, R. Tomás, J. Wenninger "IR1 and IR5 aperture at 3.5 TeV," CERN-ATS-Note-2011-110 MD (2011).

[4] S. Redaelli *et al.*, "Squeeze commissioning in IP2", MD note, in preparation.

[5] S. Redaelli, "Local aperture measurements of the triplet magnets in IR1/5 at 3.5 TeV", LHC-MD-0010 rev 0.1, EDMS 1158394.

[6] V. Baglin, N. Kos, "Beam Screens for the LHC long straight sections", LHC-VSS-ES-0002, EDMS 334961.

[7] H. Prin, private communication.

[8] Minutes of the LMC meeting of 31 August 2011.

[9] R. Bruce *et al.*, presentation at the LBOC meeting of 11 October 2011.

[10] S. Redaelli, "IR1 and IR5 aperture at 3.5 TeV", talk at the LMC, 31 August 2011.

[11] G. Müller *et al.*, "The aperture meter for the Large Hadron Collider," proceedings of ICALEPCS2011, Grenoble, FR.

[12] F. Pilat, Y. Luo, N. Malitsky, V. Ptistkin, "Beam-Based non-Linear Optics Corrections in Colliders", in 2005 Particle Accelerator Conference, ed. by C. Horak, IEEE Computer Society Press, Piscataway, 601.

[13] R. B. Appleby, J. M. Jowett, J. Uythoven, “Moving the Recombination Chambers to Replace the Tertiary Collimators in IR2”, CERN-ATS-Note-2011-014 MD.